Transient Spark Discharges in High Velocity Airflow

R. W. Macpherson, *Member IEEE*, I. V. Timoshkin, *Senior Member, IEEE*, M. P. Wilson, *Member, IEEE* and G. Burt, *Member, IEEE*

***Abstract* – Air-filled, self-breakdown plasma closing switches can operate at high pulse repetition frequency, when overstressed with HVDC voltage. However, their recovery characteristics, breakdown voltage, the achievable pulse repetition rate and variation in this rate are affected by the thermal effects local to the electrodes and by gas by-products generated by spark discharges. As a potential improvement to the performance of plasma closing switches, flowing gas can be forced through the inter-electrode gap. In this paper, it was shown that purging an inter-electrode gap of the plasma closing switch with air is a viable way of controlling the pulse repetition rate and variation of this rate. It was found that the difference between breakdown voltages of the first (single) breakdown events in static air and at 100 m/s air flow was less than 10%. In static air, the breakdown voltage of repetitive breakdown events decreases after the first and reaches its saturation value. It was shown that introduction of the air flow at 100 m/s leads to recovery of the repetitive breakdown voltage, which could reach its new saturation value, up to 30% higher than the first recorded breakdown voltage. Also, purging of the spark gap with air resulted in decreasing the pulse repetition rate, however it leads to higher breakdown voltage, lower variation in pulse repetition rate and increasing plasma conductivity in the spark channel, thereby increasing the efficiency of the overall high voltage system via reduced switching losses.**

***Index terms* – Plasma closing switch; Air flow; Breakdown voltage; Eco-friendly gas dielectrics; Repetitive operation.**

I. INTRODUCTION

In pulsed power systems, the efficiency of the switching element is of great importance when delivering energy to a load. Pulsed power applications may require a repetitive switching operation in order to drive specific loads, necessitating an efficient power/energy delivery method. The achievable pulse repetition frequency of plasma closing switches (PCS) has been of importance to researchers since the 1940s, with the energy delivered to the load dependent upon the efficiency of the PCS deployed, where fast, high-peak power switching was required. Plasma closing switches have many properties that make them suitable for pulsed power applications, including optimum voltage and current management, and low (ns or sub-ns) jitter in the triggered operational mode. However, the rate of voltage recovery after switching in simple spark gap switches is limited, which restricts their pulse repetition frequency (PRF) to a few hundred pulses per second (pps) [1].

The authors of [2] found that, in order to increase the achievable PRF of spark gap switches, an air flow between the electrodes can be introduced to remove residual charge, particles and heated gas, which could affect subsequent discharges, from the inter-electrode gap. The authors found that, with the introduction of gas flow at 36.2 m/s, the recovery time of the spark gap reduces by a factor of ~2.3 compared to that with no external air flow, for a gap of 0.91 cm. By decreasing the inter-electrode distance to 0.53 cm, the voltage recovery time was shown to be reduced by a factor of 3.8 at 36.2 m/s, compared to that with no external air flow.

The achievement of high pulse repetition frequencies using the effect of air flow on the inter-electrode gap is described in [3]. For 55 m/s air velocity, it was shown that the gas in the tested spark gap fully recovered after ~1 ms, which increased the achievable PRF of the switch to 1 kHz. When the air velocity was further increased up to 150 m/s, the recovery time decreased to 0.4 ms, enabling a pulse repetition frequency of 2.5 kHz.

In [4], the effect of air flow with velocities up to 100 m/s on the resistance of the plasma channel developed between the two sphere electrodes at breakdown is reported. The visual appearance of the plasma channels at different air velocities was investigated and the electronic temperature of plasma was estimated by the Boltzmann method, using the intensities of two copper lines in the plasma optical emission spectrum. The authors found that, when air flow was introduced, the electronic temperature was seen to increase in comparison to that with no external air flow, indicative of an increase in the conductivity of the plasma channel with increased air velocity. The visual appearance of the plasma channels varied over the range of air velocities tested also, where without air flow, the plasma channel exhibited a length of ~1 cm and a diameter of ~2 mm, but under the influence of 100 m/s air velocity, the plasma channel was stretched: its length increased up to 2 cm, and the diameter decreased to ~0.5 mm. A narrower and longer plasma channel translates to an increase in its resistance.

The influence of even higher air velocities of up to 600 m/s on DC plasma generation with surface mount rod electrodes was studied in [5 – 7], where the effect of varying air velocities up to this value was found to affect the properties of the plasma channel, particularly the critical length.

In this paper, the focus is on the breakdown and repetitive breakdown voltages measured, which is further explained in Section II, in relation to pulsed power switching, and in eco-friendly air dielectric in static (no external air flow) and in an elevated nominal flow velocity of 100 m/s. Additionally, the plasma conductivity analysis outlines the efficiency of the switching process in repetitive operation, giving insight into the different switching processes with and without airflow. It is shown that the introduction of air flow between electrodes can alter the repetitive breakdown voltages and therefore, the switching rate of the system. The generated data can be applied to the design of switching operations, to ensure the achievement of a consistent energy delivery to a load in the Hz - kHz regime, for a single-gap topology, without the

The authors are with the Institute for Energy and the Environment, Department of Electronic and Electrical Engineering, University of Strathclyde, Glasgow G1 1XW, U.K. (e-mail: ruairidh.macpherson@strath.ac.uk; igor.timoshkin@strath.ac.uk; mark.p.wilson@strath.ac.uk; graeme.burt@strath.ac.uk .

requirement for any external triggering sources. In order to characterise the temperature associated with the plasma, optical emission spectroscopy was conducted for each system configuration, to obtain the electronic temperature, and characterise the switch in terms of conductivity of plasma channels, and how these changes in relation to gap spacing, added capacitance and air velocity, thus facilitating discussion of the switching efficiency.

II. EXPERIMENTAL SETUP AND METHODOLOGY

This section details the systems and methodology associated with practical testing. The electrode configuration consisted of two 2 mm tungsten rods, with an open-air gap between. The inter-electrode gaps tested were 2 mm, 6 mm and 10 mm in length. The circuit capacitance, *C*, was also varied, through 1.35 nF, 2.7 nF and 5.4 nF, in order to characterise the effect of increased energy available in the discharge on the plasma channel characteristics, and on the plasma discharge cycle rate. The circuit diagram is shown in Fig. 1a. Using the range of 2.7 nF ceramic capacitors available, a minimum circuit capacitance of 1.35 nF was selected, on the basis that lower values resulted in the formation of a steady-state arc, rather than the desired repetitive plasma pulsations in static air. Two regimes were tested: no external air flow introduced between the electrodes (static air); and air flow with a nominal velocity of 100 m/s injected into the gap between the electrodes, with the air flow directed at 90° to a horizontally aligned electrode gap, in order for directed air flow to be aimed at the inter-electrode gap, as illustrated in Fig. 1b.

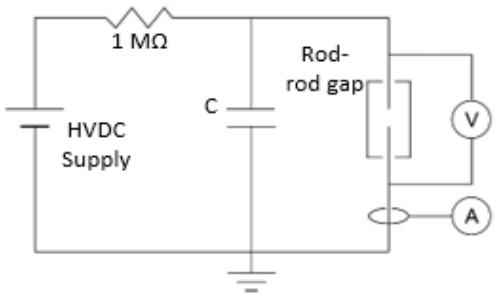

(a)

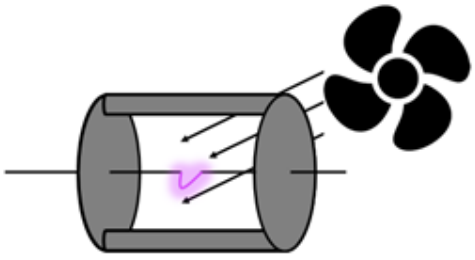

(b)

Fig. 1. a) circuit diagram b) illustration of directed air flow regime.

For the first breakdown tests, a positive polarity, 60 kV, 1.5 mA Glassman PS/EH60R01 HVDC supply was used, which was connected through a 1 MΩ charging resistor to a 2 mm diameter tungsten (high voltage) electrode. For the repetitive breakdown voltage tests, a capacitor charger, positive polarity, A.L.E TDK Lambda 802L, 50 kV, 160 mA was connected. The second tungsten rod electrode was grounded. Both tungsten electrodes had a ~60 µm radius at the edges. The circuit capacitance, *C*, was connected in parallel with the gap formed by these two rod electrodes, as shown in Fig. 1a. Two 2.7 nF, 30 kV, ceramic capacitors were used to achieve the three tested capacitances of 1.35 nF (capacitors in series), 2.7 nF (single capacitor), and 5.4 nF (capacitors in parallel). The voltage was measured by a North Star PVM-5 HV probe (80 MHz nominal bandwidth, 400 MΩ input resistance, 12 pF input capacitance) attached to the HV electrode and current was measured using a Pearson 6585 current transformer. The waveforms were monitored on a Tektronix MDO3034 oscilloscope (350 MHz bandwidth, 2.5 GS/s sampling rate). In this work, two different test methodologies were used to investigate the effects of air flow injected between the electrodes on the characteristics of plasma discharges developed in the circuit, with different capacitance and gap spacing.

Firstly, tests to characterise a single (first) breakdown event were performed, where for all parameters, the gap was stressed with an increasing voltage at a ramp rate of ~3kV/s up until the point when a breakdown event was recorded (breakdown event shown in Fig. 2). For each tested circuit condition, a total of 30 breakdown events were measured.

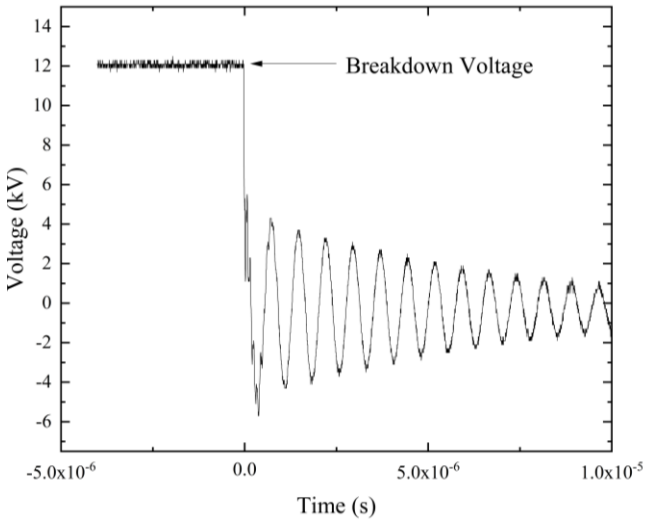

Fig. 2. Single breakdown voltage event recorded from a first breakdown test at 6 mm inter-electrode gap, with a circuit capacitance on 1.35 nF in static air. This waveform shows the single first breakdown voltage of ~12 kV.

The second test methodology was used to characterise the repetitive operation of the plasma discharge system. During these tests, the charging voltage across the gap was steadily increased at ~3kV/s until the first breakdown as shown from Fig. 3, then the system was kept energised until a regime with stable plasma pulsations (breakdowns in the air gap) was reached. This steady-state pulsation regime was achieved after a short (~15 s) relaxation time interval, in the case of no external air flow (0 m/s) at 6 mm interelectrode gap and 1.35 nF capacitance, as shown from (5) in Fig. 3. For 100 m/s however, this value was reached as soon as the air blower was energised. In the repetitive breakdown voltage operational regime, an impulsive performance was recorded from the capacitive circuit, where each discharge pulsated at a specific rate, dependent upon the circuit parameters (capacitance and

gap spacing). While for the single, first breakdown results, the applied voltage was increased until a breakdown voltage was recorded, for the repetitive breakdown voltage results, a voltage continued to be applied to the electrode system after the first breakdown event, to ensure that consistent plasma pulsation occurred, as is shown in Fig. 3.

Fig. 3 shows the breakdown voltage, defined here as being the voltage at the point of the first breakdown event (2), followed by the repetitive breakdown voltage (3), (4) and (5).

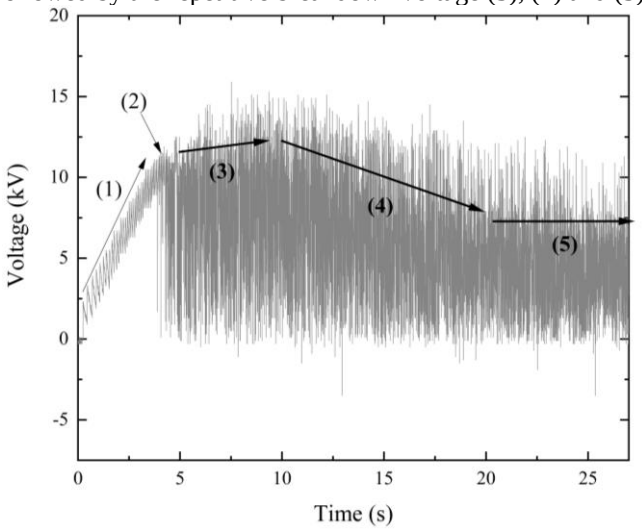

Fig. 3. Voltage across a 6 mm rod-rod gap before breakdown and after establishment of stable plasma pulsations (static air, C =1.35 nF). (1) Applied voltage increase up until first breakdown event, (2) First breakdown event at which breakdown voltage recorded, ~12 kV, (3) Unstable repetitive breakdown voltage regime after first breakdown event, (4) Repetitive breakdown voltage relaxes due to change in the electrode temperature, space charge formation and other factors, (5) Steady-state repetitive breakdown voltage regime at which repetitive breakdown voltage recorded, ~8 kV.

In the specific example shown in Fig. 3, the circuit capacitance was 1.35 nF and the inter-electrode gap was 6 mm. The behavior of the voltage with time shows the difference in the amplitude of the breakdown voltage at the first breakdown event, which is initiated after the slow ramp rate (~3 kV/s) phase associated with manually increasing the applied voltage (1), (positive DC voltage with intrinsic saw tooth ripple produced by the A.L.E supply) up to the breakdown voltage of the air gap. After the first breakdown event, (2), a repetitive breakdown regime of the system is observed (3), (4) and (5). After initial period (3), a reduction in the repetitive breakdown voltage is observed, (4) and after this period (~15 seconds following the first breakdown event, Fig. 3), the repetitive breakdown voltage begins to stabilise, (5). The time after which the repetitive breakdown voltage starts to stabilise was seen to fluctuate with different systems, therefore, recording of the repetitive breakdown voltage after ~30 seconds following the first breakdown event was the final choice for all tests, as the steady-state repetitive breakdown voltage for each system was reached by this point. In order to facilitate comparison with the 100 m/s air flow results, after the voltage reached its steady-state value in the 0 m/s regime at ~30 seconds after first breakdown (2), the air source was enabled, and the repetitive breakdown voltage was recorded after a further ~30 seconds. At 100 m/s, there was no decrease in the repetitive breakdown voltage within this timescale. From the resultant repetitive breakdown voltage waveforms produced, 30 subsequent breakdown voltages were recorded, corresponding to the maximum voltage values which were measured during this interval.

III. EXPERIMENTAL RESULTS

In Table 1, the average breakdown voltages, V_{br}, and their 2σ (two standard deviations) values for repetitive and single breakdown regimes in inter-electrode gaps ℓ =2 mm, ℓ= 6 mm, and ℓ =10 mm for C = 1.35 nF, 2.7 nF and 5.4 nF, in static air (0 m/s) and at 100 m/s air velocity. The average voltage values were obtained using 30 individual measurements for breakdown events in static air, and 30 values of steady state repetitive breakdown voltage taken from a single test run in 100 m/s air flow (region (5) in Fig. 3).

TABLE I
Single, (first) and repetitive breakdown voltages, circuit with C=1.35 nF, 2.7nF and 5.4 nF

	Air velocity (m/s)	Gap spacing (mm)	V_{br} $\pm 2\sigma$ (kV)		
			1.35 nF	**2.7 nF**	**5.4 nF**
Single (first) break-down event	0	2	8.2±0.6	8.2 ±0.6	8.2±0.7
		6	12.2±0.2	12.1±0.2	12.1±0.2
		10	14±0.3	14.3±0.6	14.2±0.5
	100	2	7.6±0.2	7.6±0.2	7.7±0.1
		6	11.7±0.2	11.8±0.2	11.8±0.2
		10	13.8±0.3	13.9±0.4	13.9±0.4
Repeti-tive break-downs	0	2	4.6±0.4	6.0±1.0	7.9±0.6
		6	7.8±0.8	9.2±0.9	8.9±0.6
		10	10±0.6	11.2±0.9	10.4±0.3
	100	2	9.9±0.8	9.4±0.7	9.3±0.5
		6	11.1±0.7	11.3±0.7	10.9±0.6
		10	16.7±1.1	15.9±0.7	15.3±0.4

Shown in Table I are the single (first) breakdown and repetitive breakdown voltages for C = 1.35 nF, 2.7 nF and 5.4 nF. At both 0 m/s and 100 m/s, as the gap distance increases, the breakdown voltage is shown to increase, as expected, for both single breakdown and repetitive breakdown modes. Analysing only the single first breakdown results, Table I shows that the difference in the average breakdown voltage at 100 m/s compared to 0 m/s is <10% for all tested inter-electrode gaps, and capacitances. Whereas for repetitive breakdown voltage operation, when the air flow is introduced to the circuit (100 m/s), the repetitive breakdown voltage of all gap distances and capacitances is shown to increase compared to that for static air (0 m/s).

For 1.35 nF, the results show a general trend that, for 0 m/s, the single first breakdown voltage is higher than the repetitive breakdown voltage, by ~78%, ~56% and ~40% for 2 mm, 6 mm and 10 mm gaps, respectively. For 100 m/s, where the average breakdown voltage in the repetitive breakdown regime is clearly higher than the single-breakdown event

regime breakdown voltage, by ~30% and ~21% for 2 mm and 10 mm gaps respectively, and a slight reduction in the mean at 100 m/s (~5% decrease), for a 6 mm gap.

For 2.7 nF, at 0 m/s, the single (first) breakdown voltage is higher than the repetitive breakdown voltage, by ~ 36%, ~32% and ~28% for 2 mm, 6 mm and 10 mm gaps, respectively. At 100 m/s, where the repetitive breakdown voltage is ~23% and ~14% higher than that for the single (first) event for 2 mm and 10 mm gaps respectively, and a slight reduction in the mean at 100 m/s (~4% decrease), for a 6 mm gap.

For 5.4 nF, in static air (0 m/s), the single (first) breakdown voltage was higher than the repetitive breakdown voltage, by ~4% for a 2 mm gap, and by ~36% for both 6 mm and 10 mm gaps respectively. At 100 m/s, the repetitive breakdown voltage was again found to be higher than that for the single (first) event, by ~21 % and ~10% for 2 mm and 10 mm gaps, but again at 6 mm, a slight reduction in the mean value (~7% decrease). Comparing all the results in Table I, it can be stated that the difference between the repetitive and single (first) breakdown voltage results is generally narrower for the higher values of capacitance.

In order to clarify how the pulse repetition frequency relates to entries for the repetitive breakdown voltage mode in Table I, Fig. 4a shows the pulse repetition frequency recorded from the 30 breakdown results for each system at 0 m/s, and Fig. 4b shows this data at 100 m/s. What is clear is that the 1.35 nF capacitance at 0 m/s results in a different operation to the other tests performed, where the achieved PRF is considerably higher than that for the other tests. As the circuit capacitance, C, is increased, with a fixed value of the charging resistor, R = 1 MΩ, the RC time constant also increases. From the RC time constants for each circuit, the corresponding level of achievable PRF, with the circuit capacitance charged to 1 RC time constant, can be calculated. For C = 1.35 nF, the RC time constant is 1.35 ms, increasing to 2.7 ms for C = 2.7 nF, and 5.4 ms for 5.4 nF. These time constants translate to nominal, calculated maximum PRF values at which C is charged to 1 RC time constant before each breakdown of 740 pps, 370 pps, and 185 pps, respectively. Considering the average values for each set of conditions, it can be seen that for C = 1.35 nF, the time interval between impulses in static air tests is: ~40% of 1 RC time constant at 2 mm, ~50% at 6 mm, and ~60% at 10 mm. At 100 m/s, however, the time interval between impulses increases and becomes longer than 1 RC time constant for all tested gaps, leading to higher energy available per pulse as compared with the tests in static air. For capacitances of 2.7 nF and 5.4 nF, however, the differences between the 0 m/s and 100 m/s pulse repetition frequencies are minimal, due to the longer time constants in comparison to those for the 1.35 nF circuit. The available charge per pulse will increase when the RC time constant is increased (i.e., when the capacitance is increased), leading to the decreasing repetitive breakdown voltages with increasing capacitance, as shown in Table I.

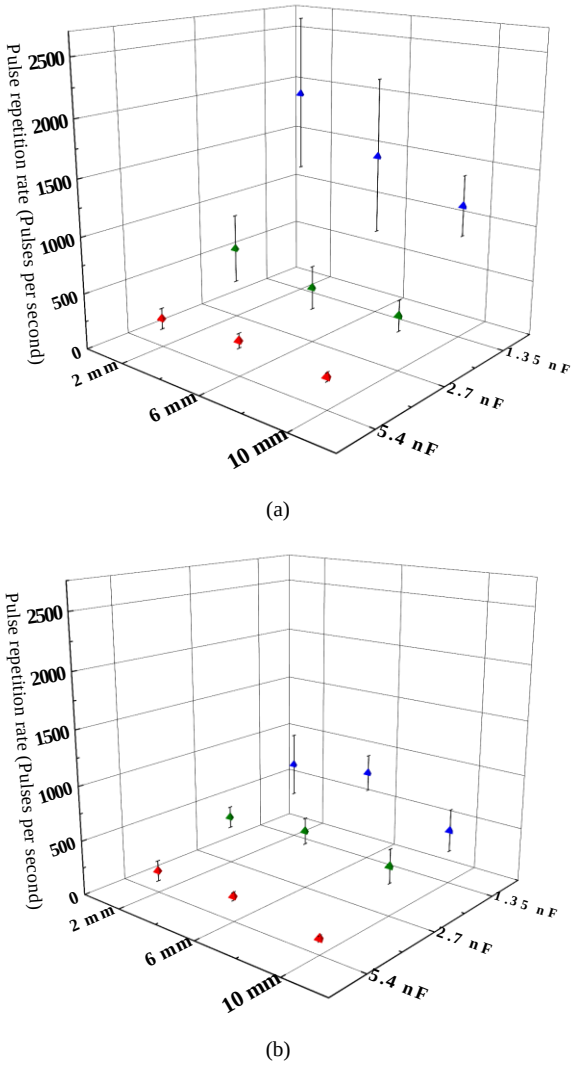

Fig. 4. Pulse repetition frequency of breakdown events at the repetitive breakdown regime for each combination of gap length and capacitance, for a) static air and b) 100 m/s air flow. Each data-point is the average of 30 individual time-to-breakdown events, error bars show the 2σ (two standard deviations) values.

IV. DISCUSSION

The minimal difference in the breakdown voltage of the system with no air flow and with 100 m/s air flow could be explained by the small change in the number density of air (molecules/volume) at 100 m/s, being only up to 5% lower than at 0 m/s, [8]. Thus, the air flow velocity of 100 m/s is considered to be the limit where the gas number density can still be considered to be the same as in static air, the upper limit of which is a maximum 5% change, essentially lowering the pressure within the flow in the inter-electrode gap, resulting in a reduction in the breakdown voltage.

When comparing single (first) and repetitive (at the repetitive breakdown voltage) breakdown, the differences in breakdown voltage can generally be attributed to two different factors: changes in local temperature and space charge accumulation. In this paper, the electronic temperature of plasma channels formed in the inter-electrode gap in repetitive

breakdown mode will be examined. In order to characterise the electronic temperature of breakdown plasma channels, optical emission spectroscopy was undertaken for each set of test conditions. This enabled extraction of the conductivity of the plasma channel during switching, in determining the efficiency of the switching process for each of the regimes tested.

The light emitted from the plasma discharge during breakdown between two copper rod electrodes directed through a fiber-optic cable into a spectrometer (OceanInsight HR2000+), and optical emission spectra were registered and analysed. The optical emission spectra of five breakdown events were captured using OceanView software and saved for analysis. With the use of copper electrodes in the test cell, Cu I emission lines at 5 different wavelengths were able to be analysed: 510.55 nm, 515.32 nm, 521.82 nm, 529.25 nm, and 578.21 nm, all easily identified in the example optical emission spectra shown in Fig. 5, for a 2 mm gap with C = 1.35 nF.

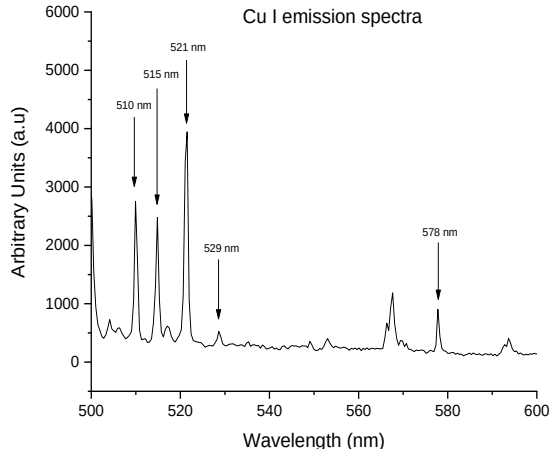

Fig. 5. Optical emission spectrum in the range 500-600 nm, from spark discharge in static air in 2 mm gap, with 1.35 nF capacitance.

The Boltzmann graph approach to obtaining the electronic temperature of plasma was selected for the purpose of this study. This approach, which is based on the assumption of local thermodynamic equilibrium (LTE) in the plasma channel, has been discussed in the literature, and found to be an appropriate method for obtaining the average plasma temperature in spark discharges [9] – [15].

In the Boltzmann graph approach, the relative peak values of the optical emission lines of specific elements are linked with the plasma temperature through Equation (1):

$$\ln\left(\frac{I_i\lambda_i}{A_i g_{iu}}\right) = \frac{E_{iu}}{k_B T} + \text{const} \qquad (1)$$

where I_i is the relative intensity of a specific emission line with the wavelength, λ_i; A_i is Einstein's transitional probability for this emission line; g_{iu} is the statistical weight of the upper level; E_{iu} is the energy of the upper level (in eV) for the specific element; k_B is Boltzmann's constant; and T is the (electronic) temperature of the plasma. The values of A_i, g_{iu} and E_{iu} are all known spectroscopic constants for specific elements, which were obtained for all relevant Cu wavelengths from the NIST Atomic Spectra Database, [16], and are shown in Table II.

TABLE II
Cu I spectral line parameters (data from [16])

Wavelength [nm]	Statistical Weight × Transition Probability [10^8 s^{-1}]	Energy Level [eV]
510.55	0.08	3.82
515.32	2.4	6.19
521.82	4.5	6.19
529.25	0.872	7.74
578.21	0.03	3.79

Using the experimental peak intensities, I_i, for the spectral lines sown in Table II, ln $((I\cdot\lambda)/(A\cdot g))$, (E_a) graphs were plotted and fitted with straight lines using Eq. (1), the slope of which can be used to find the plasma temperature, T.

An example of a Boltzmann plot is shown in Fig. 6. This Boltzmann plot was created using Eq. (1), based on the atomic Cu I lines shown in Table II observed in the optical emission spectrum (OES) of spark discharges in a 2 mm gap in static air (C = 1.35 nF). The straight line in Fig. 6 is the best fit to the experimental data, obtained using OriginPro graphing software. For each test, 5 independent OES were generated, and the best fit lines were obtained for each test. From the slope of these lines, the electronic temperature, T, was obtained by Eq. (1) for each test.

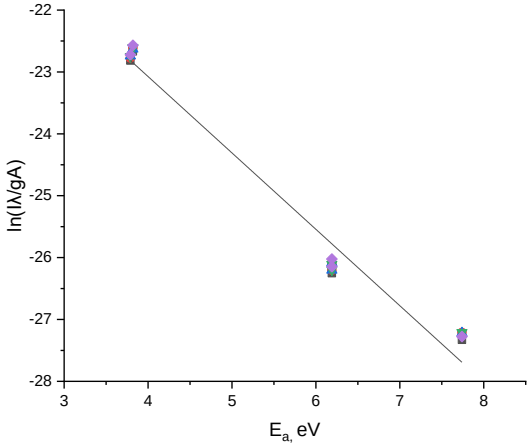

Fig. 6. Boltzmann plot obtained using Eq. (1) for the emission spectrum of 5 spark discharges in 2 mm gap in static air, C = 1.35 nF. Straight line, best linear fitting to the experimental data obtained using OriginPro graphing software.

After using this method on the data generated for all test conditions, the electronic temperatures were found, as displayed in Fig. 7. The main observation from Fig. 7 is the increase in the electronic plasma temperature with the introduction of air flow, for all combinations of circuit capacitance and gap length, and particularly for C = 5.4 nF, with a maximum increase of ~30%. At each specific gap distance, the circuit capacitance had very little effect on the electronic temperature of plasma channels obtained with no external air flow (0 m/s). When the air flow is injected into the inter-electrode gap (100 m/s), however, a slight upwards trend was recorded. It was observed that, with an increase in gap spacing, there was also an increase in the electronic temperature of the plasma.

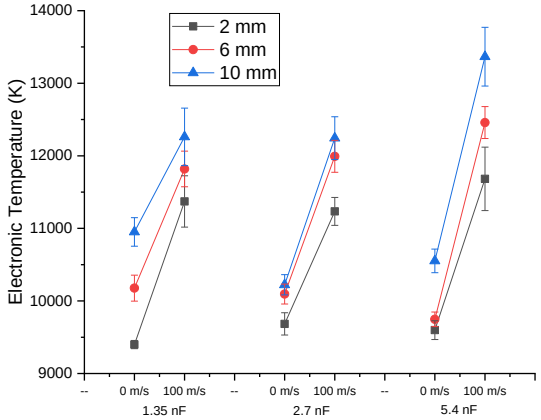

Fig. 7. Electronic temperature of plasma in the discharge channel for all test conditions. Each data-point is the average of 5 individual breakdown events, with the 1σ (one standard deviation) values shown in the form of error bars. Straight connecting lines are for visual guidance only.

The plasma conductivity can be calculated using the Spitzer equation, Eq. (2), assuming that the plasma is in LTE, and that the ionic charge is equal to the electronic charge, [17]:

$$\sigma = \frac{0.582 \cdot T^{\frac{3}{2}}}{38 \cdot \ln\left(1.24 \cdot 10^{7} \cdot T^{\frac{3}{2}}/\sqrt{n_e}\right)} \qquad (2)$$

where, T is the (electronic) temperature of the plasma (K), measured using the Boltzmann plot method illustrated in Fig. 6, and n_e is the concentration of electrons in the channel (1/m^3). Here, the value of n_e in Eq. (2) was either 10^{20} 1/ m^3 or 10^{22} 1/ m^3, to give two different values of conductivity for each test. From the temperature results presented in Fig. 7, it was found that in the case of static air, the conductivity of the plasma channel (found using Eq. (2)), was in the range 1,900-3,100 S/m. At 100 m/s, the conductivity of the plasma channel was found to be in the range 2,700-3,900 S/m. For both static air and 100 m/s tests, the conductivity followed an increasing trend with increasing gap distance and circuit capacitance.

The conductivity which is measured in Section IV may give information on the plasma resistance of the switch, which will have an effect on the voltage collapse across the switch during closure. Also, knowing the conductivity values could give information on the total energy which is injected into the plasma channel and any energy losses during the switching process. The increase in electronic temperature shown at 100 m/s may determine that the conductivity of the plasma discharge increases, which therefore minimises the plasma resistance, increasing the efficiency of the energy transfer. In the case of fast switching operations, these parameters are important in order to enable efficient operation of a pulsed power system, as the transient time is at its minimum value, during which the plasma discharge conductivity increases to its maximum value.

These differences in plasma conductivity will also have an effect on the temperature distribution as a whole, particularly with the tungsten electrodes used in the main tests reported in Section III. Shown in Fig. 8 are images illustrating the appearance of the plasma for each combination of gap length and capacitance, in 100 m/s air flow. These stills taken from video imaging of the plasma discharges were obtained using a Sony DSC-RX10 IV camera. From these images, it can be seen that the plasma channel morphology tends to change with increasing gap spacing. This change may have an effect on the current density throughout the plasma channel, and therefore the temperature distribution. At larger radius, >1 mm (radii of electrode), the current density will be focused on the electrode, which could result in a local increase in temperature.

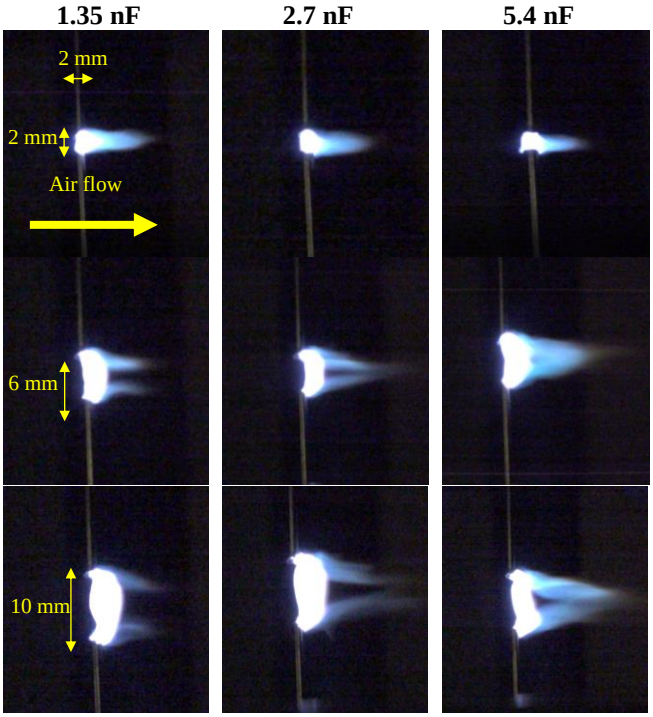

Fig. 8. Visual appearance of plasma channel(s) at 100 m/s air velocity for all tested combinations of gap length and capacitance. Still shots from video were obtained using a Sony DSC-RX10 IV camera, at 120 fps.

The reduction in the repetitive breakdown voltages compared to the single (first) breakdown voltages in static air (at 0 m/s) in Table I, could be explained by the presence of residual charge, left behind during the repetitive plasma operation. This behaviour is evident for all conditions, but particularly for the 2 mm inter-electrode gap, where the repetitive breakdown voltage decreases by up to 44% for the circuit with C = 1.35 nF, 27% for C = 2.7 nF and 4% for C = 5.4 nF. For the tests with a 2 mm gap at 0 m/s, the electronic temperature shown is at a value of ~9,500 K, yielding a plasma conductivity in the range 2,000 – 3,000 S/m, irrespective of circuit capacitance. However, it can be seen that, for the tests with C = 1.35 nF at 2 mm, the pulse repetition frequency recorded was higher than that for the tests with C = 2.7 nF and C = 5.4 nF. Therefore, it is hypothesised that this could be the dominant factor in determining the repetitive breakdown voltage, as higher pulse repetition frequency could increase the concentration of charged species within the gap, ultimately lowering the repetitive breakdown voltage over time. This effect has also been observed in [18] and [19].

Shown in [18], the pre-ionization level of ensuing discharges is closely correlated with the pulse repetition frequency, where a breakdown event is easier to accomplish at high pulse repetition frequency, since the number of applied pulses before

breakdown lowers as PRF rises. The authors show that the accumulation effect, which is caused by excited metastable particles and residual charges from successive nanosecond pulses, is closely connected to the breakdown voltage of the system. Additionally, repetitive pulsed discharges were studied experimentally and theoretically by Huang et al, [19], with a focus on the effects of PRF on discharge characteristics. The authors found that the large residual charge density at a high PRF tended to lower the breakdown voltage, the peak power, and the peak electron density in the pin-to-pin electrode arrangement tested. With increasing pulse repetition rate, the the electron density and the electron temperature were higher nearer the cathode, so that residual charges during the breakdown period had an impact on how energetic electrons and electric fields were distributed across the electrodes.

For gaps of 6 mm and 10 mm, with the 1.35 nF and 2.7 nF capacitances at 0 m/s, the plasma pulse repetition frequency was found to decrease in comparison to that for the corresponding tests with a gap of 2 mm. With longer gap spacing, it can be assumed that, for each breakdown event within the repetitive operation region, the charge deposited will be higher, as the breakdown voltage is increased in relation to gap distance, as shown in Table I. However, due to the lower pulse repetition frequency at longer gap lengths, the accumulation of residual charges left behind by successive discharge events is not so pronounced. Therefore, the difference between the single (first) breakdown voltage and repetitive breakdown voltage decreases. For C = 5.4 nF, as the gap increased, the difference between the single (first) breakdown voltage and repetitive breakdown voltage was found to increase. This is hypothesised as being due to the synergistic effects of pulse repetition frequency, higher charge per pulse and the gap distance having an effect on charge accumulation, impacting upon the breakdown voltage. Furthermore, as the gap spacing increases to 6 mm and 10 mm, the change in capacitance is shown to have a lesser effect on the pulse repetition frequency of the system, where the pulse repetition frequency is similar for 1.35 nF, 2.7 nF and 5.4 nF, at both 6 mm and 10 mm. This results in the difference between the repetitive breakdown voltage and the single (first) breakdown voltage becoming less pronounced as the capacitance is increased for these gap lengths. For a 6 mm gap, the repetitive breakdown voltage decreased by 37% for C = 1.35 nF, by 25% for C = 2.7 nF, and by 26% for C = 5.4 nF. For a 10 mm gap, the repetitive breakdown voltage decreased by 29% for C = 1.35 nF, by 22% for C = 2.7 nF, and by 27% for C = 5.4 nF.

With introduced air flow, the electronic temperature was shown to increase for each set of test conditions, when increasing from 0 m/s (no air flow) to 100 m/s air velocity, as shown in Fig. 7. However, in this arrangement, this results in a higher breakdown voltage for each test, where the repetitive breakdown voltages increase compared to the single (first) event breakdown voltages, as shown in Table I. Relating this to the previous discussion in Section IV, under high pulse repetition frequency conditions, the residual charges left behind from successive breakdown events are essentially swept away by the high air velocity, which then requires a higher applied voltage to initiate breakdown of the gap. Another reason for this behaviour could be due to the gas flow assisting the neutral particles in leaving the plasma zone, causing a fall in particle density, which in turn suppresses the spark and causes the discharge to switch to the diffuse mode, associated with an increase in the breakdown voltage with increasing air flow, [20].

Therefore, it is hypothesised that one of the factors in determining the change in the repetitive breakdown voltage, in comparison to the single (first) breakdown voltage, is the residual charges which are left behind by subsequent discharges. As aforementioned, for single (first) breakdown results, there was no significant change in breakdown voltage at 100 m/s compared to the static air case (0 m/s), potentially due to minimal charge accumulation at the electrodes between breakdown events, as each subsequent breakdown was triggered after 10s of seconds. In repetitive breakdown voltage mode, when the pulse repetition frequency increases, the breakdown voltage of the system in the static air decreases. At 100 m/s, a sweeping effect was introduced on the electrode system by the added air velocity and therefore the repetitive breakdown voltage increased in comparison to that for the single (first) breakdown voltage event.

V. CONCLUSION

In this paper, an investigation into the utilisation of an environmentally friendly dielectric fluid (gas), in the form of flowing atmospheric air, to enable repetitive switching operations in pulsed power systems was conducted, in order to facilitate the substitution of high carbon footprint gases which are prevalent in the high voltage and pulsed power sectors [21], [22]. Baseline data in static air (no external air flow) was gathered and compared with that obtained when 100 m/s air flow was introduced into the inter-electrode gap, with varying circuit capacitance and gap length. It was shown that the air flow affected the breakdown voltage and pulse repetition frequency. The outlined key aspects of this paper are that, for repetitive operation at 0 m/s, the breakdown voltage decreases to a minimum value, which ultimately increases the pulse repetition rate of the switch. Purging the 2 mm and 10 mm inter-electrode gaps with atmospheric air at 100 m/s facilitates an increase in the breakdown voltage of repetitive breakdowns, compared to the first breakdown event. At the same time, the airflow also had the effect of reducing the overall achieved pulse repetition rate. Nevertheless, it was shown that the increased breakdown voltage in the case of 100 m/s airflow results in the increased conductivity of the plasma channels formed in the gap, enabling higher overall efficiency of the switch, via reduced switching losses. Therefore, dependent upon the application, the energy delivered from the capacitive circuit can be tailored by changing the circuit parameters and environmental conditions, to prioritise either higher pulse repetition rate, or higher system efficiency.

Further work will consist of thermal modelling of the electrode system using the obtained conductivities of the plasma channels, in order to characterise the temperature distribution within the different plasma topologies and the overall electrode system over time.

REFERENCES

[1] C. S. Reddy, A. S. Patel, P. Naresh, Archana Sharma, and K. C. Mittal, "Experimental investigations of argon spark gap recovery times by developing a high voltage double pulse generator", *Review of Scientific*

Instruments, American Institute of Physics, vol. 85, no. 6, June 2014 doi:10.1063/1.4883997
[2] J. M. Kuhlman, G. M. Molen, "Performance of high-power gas-flow spark gaps", *American Institute of Aeronautics and Astronautics*, vol. 24, no. 7, 1986, doi:10.2514/3.9400
[3] W. J. Thayer, V. C. H. Lo, and A. K. Cousins, "Recovery of a high pulse rate spark gap switch," *IEEE Conference Record of the 1988 Eighteenth Power Modulator Symposium*, Hilton Head, SC, USA, 1988 pp. 257-264, doi: 10.1109/MODSYM.1988.26281.
[4] L. Xiaoang Y. Zhang, C. Ma, *and* L. Liu , "Spark resistance under high-speed gas flow in the oscillatory damped regime of discharge*", Physics of Plasmas, American Institute of Physics*, vol. 25, no. 6, 2018 https://doi.org/10.1063/1.5043312
[5] V. M. Shibkov, L. Shibkova, and A. A. Logunov, "Effect of the Air Flow Velocity on the Characteristics of a Pulsating Discharge Produced by a DC Power Source". *Plasma Physics Reports*. vol. 44, no. 8. pp. 754-765, 2018, doi:10.1134/S1063780X18080056.
[6] A. A. Logunov,K. N. Kornev, . L. V. Shibkova, and V. M. Shibkov, V. "Influence of the Interelectrode Gap on the Main Characteristics of a Pulsating Transverse-Longitudinal Discharge in High-Velocity Multicomponent Gas Flows." *High Temperature*. vol. 59, no. 1, pp. 19-26, 2021, doi: 10.1134/S0018151X21010119.
[7] V.M Shibkov, K.N. Kornev, A.A. Logunov, and Y. K. Nesterenko, "Gas Heating under Conditions of Pulsating Transverse–Longitudinal Discharge in Subsonic and Supersonic Airflows." *Plasma Phys. Rep.* vol. 48, no. 7 pp. 798–805, 2022. doi: 10.1134/S1063780X22700246
[8] S. Asao, M. Yamakawa, K. Sawanoi, and S. Takeuchi, "Flight Simulation of Water Rocket" *International Journal of Computational Methods*, Special Issue: ICCM 2020, World Scientific Publishing Co**.** vol. 19, no. 7, doi:10.1142/S0219876221410176
[9] A. Sarani, A. Y. Nikiforov, and C. Leys, "Atmospheric pressure plasma jet in Ar and Ar/H2O mixtures: Optical emission spectroscopy and temperature measurements", *Phys. Plasmas*, vol. 17, no. 6, 2010, https://doi.org/10.1063/1.3439685
[10] V. K. Unnikrishnan, K. Alti, V. B. Kartha, C. Santosh, G. P. Gupta, and B. M. Suri. "Measurements of plasma temperature and electron density in laser-induced copper plasma by time-resolved spectroscopy of neutral atom and ion emissions". *Pramana - J Phys*, vol. 74, no. 6, pp. 983–993 2010, doi:10.1007/s12043-010-0089-5
[11] I. Prysiazhnevych, V. Chernyak, S. Olzewski, and V. Yukhymenko, "Plasma properties of transverse blowing arc under atmospheric pressure," *Chem. List*., vol. 102, no. 16, pp. 1403–1407, 2008.
[12] S. Gershman, A. Belkind and K. Becker, "Optical emission diagnostics of the plasma channel in a pulsed electrical discharge in a gas bubble," *2009 IEEE Pulsed Power Conference*, Washington, DC, USA, 2009, pp. 838-843, doi: 10.1109/PPC.2009.5386370.
[13] N. Zhang, F. Sun,L. Zhu, M. P. Planche,H. Liao,C. Dong,and C. Coddet, "Electron Temperature and Density of the Plasma Measured by Optical Emission Spectroscopy in VLPPS Conditions" *Journal of Thermal Spray Technology*, vol. 20 pp. 1321 – 1327, 2011-doi: 10.1007/s11666-011-9681-6. T.
[14] T. Billoux, V. Boretskij, Y. Cressault, A. Gleizes, P. Teulet, and A. Veklich, "Emission spectrum of the electric arc discharge in CO 2 between copper electrodes," *Proc. International Symposium Plasma Chemistry (ISPC)* 2013, pp. 1–4.
[15] C. O. Laux, T. G. Spence, C. H. Kruger and R. N. Zare, "Optical diagnostics of atmospheric pressure air plasmas," *Plasma Sources Sci. Technol.*, vol. 12, no. 2, pp. 125 - 138, 2003, doi:10.1088/0963-0252/12/2/301
[16] NIST Atomic Spectra Database - 'https://www.nist.gov/pml/atomic-spectra-database' Visited 9th May 2023.
[17] R. Zollweg and R. W. Liebermann, "Electrical conductivity of non-ideal plasmas", *Journal of Applied Physics, American Institute of Physics*,vol. 62, no. 9, pp. 3621 – 3627, 1987, doi:10.1063/1.339265
[18] T. Shao, G. Sun, P. Yan, W. Jue, Y. Weiqun, S. Yaohong and Z. Shichang 'An experimental investigation of repetitive nanosecond-pulse breakdown in air', *J. Phys. D, Appl. Phys*., vol. 39, no. 10, pp. 2192 – 2197, 2006, doi:10.1088/0022-3727/39/10/030
[19] B. Huang, K. Takashima, X. Zhu, Y. Pu, 'The influence of the repetition rate on the nanosecond pulsed pin-to-pin micro discharges', *J. Phys. D, Appl.Phys*., IOP Publishing, vol. 47, no. 42, 2014 doi: 10.1088/0022-3727/47/42/422003
[20] C. Zhang, T. Shao, P. Yan, and Y. Zhou, "Nanosecond-pulse gliding discharges between point-to-point electrodes in open air". *Plasma Sources Science and Technology*. vol. 23. no. 3, 2014, 035004. doi: 10.1088/0963-0252/23/3/035004.
[21] M. Eves, D. Kilpatrick and P Edwards. "A Literature Review on SF6 Gas Alternatives for use on the Distribution Network." *Next Generation Networks*, Western Power Distribution, 2018. Available online: https://www.westernpower.co.uk/downloads/5857 (accessed on 17 May 2023).
[22] M. Wisher, O. Johns, E. Breden, J. Calhoun, F. Gruner, R. Hohlfelder, T. Mulville, D. Muron, B. Stoltzfus, and W. Stygar, "Field-Distortion Air-Insulated Switches for Next-Generation Pulsed-Power Accelerators*". Sandia National Lab* United States: 2017. Web. doi:10.2172/1395749.

Ruairidh W. Macpherson (M'23) was born in Inverness, Scotland, in 1990. He received his B.Eng. (Hons.), MPhil and PhD degrees from the University of Strathclyde in 2016, 2019 and 2023 respectively. Where he is currently working with the High Voltage Technologies Group, Department of Electronic and Electrical Engineering. His research interests include work in pulsed power technologies, corona-stabilised switches, environmentally friendly gas dielectrics, surface flashover of gas-solid interfaces within sub-optimal environmental conditions and HVAC, HVDC and impulsive plasma characterisation.

Igor V. Timoshkin (M'07–SM'14) received the degree in physics from Moscow State University, Moscow, Russia, in 1992, and the Ph.D. degree from the Imperial College of Science, Technology, and Medicine (ICSTM), London, U.K., in 2001. He was a Researcher with Moscow State Agro-Engineering University, Moscow, and the Institute for High Temperatures of the Russian Academy of Sciences, Moscow. In 1997, he joined ICSTM. He joined the Department of Electronic and Electrical Engineering, University of Strathclyde, Glasgow, U.K., in 2001, where he became a Reader in 2016. His research interests include dielectric materials, pulsed power, transient spark discharges, and environmental applications of non-thermal plasma discharges. Dr. Timoshkin was a Voting Member of the Pulsed Power Science and Technology Committee in the IEEE Nuclear and Plasma Science Society (2017–2021); currently he is a member of the International Advisory Committee of the IEEE Conference on Dielectric Liquids and the International Scientific Committee of the Gas Discharges and their Applications Conference; a Subject Editor of IET Nanodielectrics and a member of the Editorial Board of MDPI Energies.

Mark P. Wilson (M'10) was born in Stranraer, Scotland, in 1982. He received the B.Eng. (with honours), M.Phil., and Ph.D. degrees in electronic and electrical engineering from the University of Strathclyde, Glasgow, U.K., in 2004, 2007, and 2011, respectively. He is presently based in the High Voltage Technologies research group at the University of Strathclyde, where his research interests include interfacial surface flashover, nanodielectrics, and the practical applications of high-power ultrasound, corona discharges, and pulsed electric fields. Mark is a member of the IEEE Nuclear and Plasma Sciences Society, from whom he received a Graduate Scholarship Award in 2011, the IEEE Dielectrics and Electrical Insulation Society, and the IET.

Graeme M. Burt (M'95) received the B.Eng. degree in electrical and electronic engineering, and the Ph.D. degree in fault diagnostics in power system networks from the University of Strathclyde, Glasgow, U.K., in 1988 and 1992, respectively. He is a distinguished professor of electrical power systems in the Department of Electronic and Electrical Engineering at the University of Strathclyde, UK, where he directs the Institute for Energy and Environment. His research interests span decentralised and hybrid energy systems, electrification of propulsion, and experimental validation of advanced power systems. Professor Burt is lead academic for the PNDC, a MW-scale innovation and testing infrastructure, and director of the Rolls-Royce UTC in Electrical Power Systems. He serves on the IEEE TF on Cloud-Based Control and Co-Simulation of Multi-Party Resources in Energy Internet, the CIRED WG for DC Distribution Networks, EERA JP in Smart Grids, SAB of the Clean Aviation Joint Undertaking, and the Board of the Association of European Distributed Energy Resources Laboratories (DERlab eV.).